Anal. Bioanal. Electrochem., Vol. 4, No. 4, 2012, 342 - 356

Analytical & Bioanalytical Electrochemistry

Full Paper

Direct Electrochemistry and Electrocatalysis of Myoglobin Immobilized on a Novel Chitosan-Nickel Hydroxide Nanoparticles-Carbon Nanotubes Biocomposite Modified Glassy Carbon Electrode

Ali Babaei[1,2*] and Ali Reza Taheri[1]

[1]*Department of Chemistry, Faculty of Science, Arak University, Arak, 38156-8-8349, Iran*
[2]*Research Center for Nanotechnology, Arak University, Arak, 38156-8-8349, Iran*

*Corresponding Author, Tel.: +98 861 4173401; Fax: +98 861 4173406

E-Mail:a-babaei@araku.ac.ir, ali.babaei08@gmail.com

Received: 28 July 2012 / Accepted: 14 August 2012 / Published online: 27 August 2012

Abstract- A novel myoglobin-based electrochemical biosensor was developed. The fabricated biosensor is based on a nanobiocomposite prepared from multiwalled carbon nanotubes and $Ni(OH)_2$ nanoparticles that were coated with myoglobin and chitosan. Cyclic voltammogram of the electrode showed a pair of well-defined and quasi-reversible redox peaks with a formal potential ($E^{0'}$) of –0.330 V in 0.1 M pH=7.5 phosphate buffer solution, which was the characteristic of the Mb heme Fe(III)/Fe(II) redox couple. Immobilized Mb exhibits excellent electrocatalytic activity toward the reduction of hydrogen peroxide. The linear range for the determination of hydrogen peroxide was from 0.4 to 702 μM with a detection limit of 0.08 μM using chronoamperometry method. The kinetic parameters such as the electron transfer coefficient and the heterogeneous electron transfer rate constant for H_2O_2 determination were determined using electrochemical approaches. The biosensor was used for determination of H_2O_2 in human blood serum and the oxidant with satisfactory results.

Keywords- $Ni(OH)_2$ Nanoparticles, Carbon Nanotubes, Chitosan, Electrochemical Biosensor

1. INTRODUCTION

Direct electrochemistry of most redox proteins on conventional electrodes is a great challenge due to the deeply buried redox-active center inside the proteins [1]. Moreover, the denaturation and loss of electrochemical activities will occur when the proteins adsorbed directly on the electrode surface [2]. Thus, one of the main challenges in this area is to develop a host matrix which can both provide a suitable microenvironment for proteins and also enhance direct electron transfer between their redox-active center and underlying electrodes. Myoglobin (Mb), a kind of oxygen transportation protein with the function to store and transport oxygen, has an active heme redox center.

The oxidation of some biological substances in body can produce certain amounts of H_2O_2. The content of H_2O_2 is also related with the environmental chemistry. Furthermore, hydrogen peroxide and its derivatives are powerful oxidizing agents, which can therefore be employed in the synthesis of many organic compounds [3]. So it is of great importance to establish sensitive and convenient methods for H_2O_2 detection. Detection of hydrogen peroxide which is a byproduct in an enzymatic reaction is important in the field of biosensor fabrication [4].

Carbon nanotubes (CNTs) as a type of nanomaterials have attracted attention during recent years [5]. CNTs can be coupled to enzymes to act as electrical connectors between the redox center of the enzymes and the electrodes [6]. In recent years, many studies focused on the direct electrochemistry of proteins which were incorporated into the composites to investigate the stability and biocompatibility of films. These films contained water-insoluble surfactants [7, 8], hydrogel polymers [8], polyelectrolyte- or clay-surfactant composites [9], Chitosan [10], nanoparticles [11] and MWCNTs [12]. Immobilizing proteins or enzymes with nanoparticles has become a popular surface derivatization procedure; the reason for this is mostly ascribed to its easy preparation and versatility and to the establishment of a high level of order on a molecular scale [13]. The film formed by this technique has the advantages of high organization and uniformity, which could provide a desirable microenvironment to immobilize protein and facilitate the direct electron transfer from the protein to the underlying electrode. In particular, transition-metal nanoparticles, in different forms, have emerged as a novel family of catalysts able to promote more efficiently a variety of organic transformations because of their small size and extremely large surface-to-volume ratio [14, 15]. Some nanoparticles have been successfully introduced onto CNTs, such as CdTe [16], Au [17], Cu [18] and Ag [19]. Many electrodes were modified by Ni, NiO_2, $Ni(OH)_2$ particles and nanoparticles on traditional electrode surfaces such as diamond [20], gold [21], carbon or graphite [22-24]. In contrast to Ni nanomaterials which are unstable and easily oxidized in air and solution, hydroxide (or oxide) of this material is relatively stable [22, 23, 25].

Nickel hydroxide with a small crystalline size shows a high proton diffusion coefficient, giving excellent electrochemical performance. many precipitation methods for preparing Nano scale nickel hydroxide such as coordination precipitation, precipitation transformation, hydrothermal conversion, urea homogeneous precipitation, micro emulsion, need harsh reaction conditions such as high temperature or pressure; some need organic solvent, which increases the production cost; and some need the addition of extra precipitator to the reaction system, which the precipitator is readily partially over concentrated, and thus resulting in poor quality of this production [23,25-28]. However, the method of coordination homogeneous precipitation is new and facile, needing no expensive raw materials or equipment, it is also easy for mass production, and can be extended to synthesize other hydroxide or oxide nanocrystals.

Chitosan (Cs) is a transformed polysaccharide obtained by deacetylation of natural chitin, which is one of the naturally occurring biopolymers and widely present in the exoskeleton of crustaceans and other biological materials [29]. Due to its desirable properties such as low cost, chemical inertness, high mechanical strength, high hydrophilicity, and good film-forming ability, chitosan has been used in various practical fields. A distinct advantage of chitosan in fabricating biosensors is its MWCNTs biocompatibility and nontoxicity. We thus expect that Cs films may provide a suitable microenvironment for redox proteins to exchange electrons with underlying electrodes directly. Herein, we developed a composite biofilm, which contains MWCNTs, $Ni(OH)_2$ nanoparticles, Cs and Mb, based on the idea that the MWCNTs with $Ni(OH)_2$ nanoparticles could facilitate the electron transfer and Cs had good biocompatibility and stability.

2. EXPERIMENTAL

2.1. Reagents and solutions

Horse heart myoglobin (Mb, MW 17,800), was purchased from Sigma and used as received. Multi-walled carbon nanotubes (MWCNTs) (>95 wt%, 5-20 nm) was purchased from PlasmaChem GmbH company. Chitosan (CS) (MW: 20,0000) was dissolved in acetic acid (1.0 g chitosan in 100 ml 0.05 M acetic acid). A 30% H_2O_2 solution was purchased from Sigma Chemical Company and the concentration of H_2O_2 solution was determined by titration with standard $KMnO_4$ solution. 0.1 M Phosphate buffer solution (PBS) was prepared by dissolving appropriate amounts of disodium hydrogen phosphate and sodium dihydrogen phosphate in 250 mL volumetric flask. Fresh human serum samples were available from Razi Institute of Vaccine and Serum Company (Tehran, Iran).

2.2. Synthesis of nanoscale $Ni(OH)_2$

Nanoscale $Ni(OH)_2$ was synthesized using a coordination precipitation procedure as previously reported [26]. Briefly, by adding concentrated ammonia (28wt.%) to nickel nitrate solution (1 M), a deep blue colored nickel hexamine complex solution was formed and added into a given amount of distilled water, the reaction was carried out under magnetic stirring for 1 h at 70 ^oC. Finally, light green sediments were formed. The precipitate was separated by centrifuge and rinsed with distilled water and ethanol three times respectively to remove the adsorbed ions, then dried in a vacuum oven at 80 ^oC for 12 h; the final product was green powder. Product that is obtained without any surfactant in the reaction process was platelet-like shape. The method is simple and facile; it is low cost and also easy for mass production and can be extended to synthesize other hydroxide or oxide nanocrystals.

2.3. Instrumentation

All the voltammetric measurements were carried out using Cs/Mb/$Ni(OH)_2$-MWCNTs/GCE as the working electrode, Ag/AgCl, 3 M KCl as the reference electrode and platinum wire as an auxiliary electrode. Cyclic voltammetry (CV) and chronoamperometry (CA) experiments were carried out in oxygen free water under nitrogen by using an Autolab PGSTAT 30 Potentiostat Galvanostat (EcoChemie, The Netherlands) coupled with a 663 VA stand (Metrohm Switzerland). The pH measurements were performed with a Metrohm 744 pH meter using a combination glass electrode.

2.4. Fabrication of H_2O_2 biosensor

Prior to use, the glassy carbon electrode (2 mm in diameter) was first polished with alumina slurry (followed by 1.0 μm and 0.05 μm) and ultrasonically cleaned with 1:1 water, ethanol and distillated water. A stock solution of MWCNTs–$Ni(OH)_2$ in DMF was prepared by dispersing weighed amounts of MWCNTs and $Ni(OH)_2$ nanoscale (95%:5% w/w) in 1 mL DMF using ultrasonic bath until a homogeneous solution resulted, and 20 μL of prepared suspension was casted on the electrode with a microsyring. The electrode was dried in air, denoted as MWCNTs-$Ni(OH)_2$/GCE.10 μL of 15 mg/mL Mb was dropped on the modified GCE surface, and allowed to dry under ambient conditions for 3 h. After that, 5 μL of chitosan solution was casted on the surface of the electrode and was set in ultrasonic bath to form a stable composite film. The fabricated electrode was denoted as Cs/Mb/$Ni(OH)_2$-MWCNTs/GCE and stored at 4 ^oC when not in use. Fig. 1 shows the Schematic illustration of stepwise Electrode modification. For comparison, Cs/Mb/$Ni(OH)_2$/GCE, Cs/Mb/MWCNTs/GCE, MWCNTs/GCE and $Ni(OH)_2$-MWCNTs/GCE were prepared and used for further investigation.

2.5. General procedure

10 mL solution containing appropriate amounts of H_2O_2 in 0.1 M PBS at pH 7.5 was transferred into the voltammetric cell. Calibration curves were obtained by plotting the cathodic peak currents of H_2O_2 against the corresponding concentrations. All experiments were carried out under open circuit conditions.

After each measurement, the electrode was regenerated by thoroughly washing the electrode with distilled water and then 0.5% sodium hydroxide solution. The electrode was finally rinsed carefully with distilled water to remove all adsorbate from electrode surface and provide a fresh surface for next experiment.

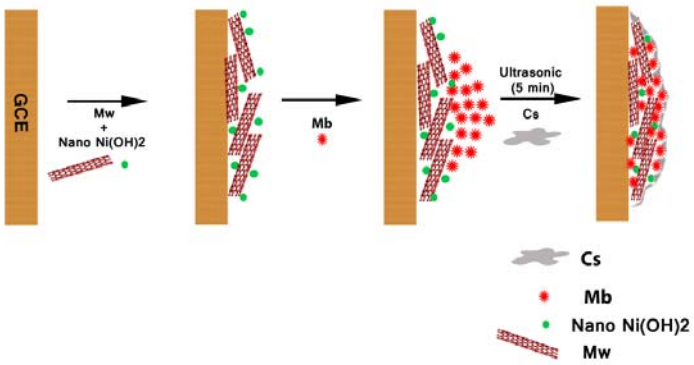

Fig. 1. Schematic illustration of stepwise fabrication process of biosensor: Cs/Mb/$Ni(OH)_2$-MWCNTs/GCE

3.RESULT AND DISCUSSION

3.1. Characterization of the electrode

In order to study the electrode surface, different parts of the electrode surface were observed by scanning electron microscopy (SEM). Fig. 2 shows a typical image of the MWCNTs and $Ni(OH)_2$ nanoscale synthesized through coordination precipitation method. It shows a platelet-like nanostructure with a dimension in the range of 50–100 nm. It can be seen that, size-homogeneity of these particles is very well.

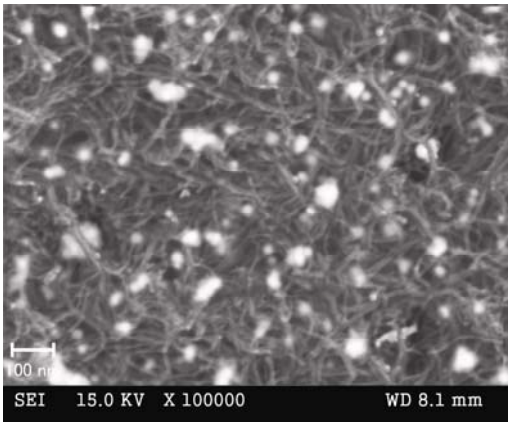

Fig. 2. SEM image of the MWCNTs and $Ni(OH)_2$ nanoscale on glassy carbon

3.2. Electrochemical behavior of Cs/Mb/$Ni(OH)_2$–MWCNTs/GCE

In order to investigate the electrochemical properties of Cs/Mb/$Ni(OH)_2$-MWCNTs modified electrode, cyclic voltammograms were recorded in phosphate buffer solution. As shown in Fig. 3b, no redox peaks can be seen for $Ni(OH)_2$-MWCNTs/GCE in the potential range of -1 to 0.3 V, indicating that there were no electroactive substances to react at this range and the redox peaks should be attributed to Mb electron transfer on electrode. Electron transfer between Mb and electrode was facilitated by $Ni(OH)_2$ nanoparticles imbedded in the complex film as a result of the nano-size effect of $Ni(OH)_2$ nanoparticles (Fig. 3a). On the other hand, if the MWCNTs and Mb mixture was dropped on the electrode could provide a desirable microenvironment to immobilize protein and facilitate the direct electron transfer from the protein to the underlying electrode (Fig. 3c). However, for Cs/Mb/$Ni(OH)_2$-MWCNTs/GCE (Fig. 3d) a pair of reduction–oxidation peaks with formal potential -0.33 V and the peak-to-peak separation (ΔE_p) was calculated to be 95 mV at a scan rate of 100 mV/s, indicating a fast and quasi-reversible electron transfer process. The ratio of anodic to cathodic peak currents is about one. This also indicates that myoglobin undergoes a quasi-reversible redox process at the glassy carbon electrode modified with Cs/Mb/$Ni(OH)_2$-MWCNTs film. Thus, the film must have a great effect on the kinetics of electrode reaction and provide a suitable environment for the myoglobin to transfer electron with the underlying GC electrode. The shapes of anodic to cathodic peaks were nearly symmetric, and the heights of reduction and oxidation peaks are the same. This behavior suggests that all of the electroactive MbFe(III) within the film are converted to MbFe(II) on the forward scan to negative potential and vice versa. Herein, CS was adopted to fix Mb on the electrode; meanwhile, adding Cs into Mb can also improve the adherence of the composite film with the electrode surface.

3.3. Optimization of Experimental Variables

The influence of amount of immobilized Mb on the analytical characteristics of the enzyme electrode was studied. Fig. 4A displays the effect of the amount of Mb enzyme in the modified electrode. The current response increases sharply as the protein amount increases and reaches maximum at 15 mg mL^{-1}, and then the current did not change significantly with further increase of the Mb concentration. Such a behavior is typical of a mediator-based sensor [30]. So, an optimum loading 10 μL of 15 mg mL^{-1} Mb was used for subsequent experiment.

Modification of GCE with different amounts of MWCNTs and $Ni(OH)_2$ nanoscale was tested for evaluation the electrochemical response of Mb by cyclic voltammetry. It was found that as the ratio of $Ni(OH)_2$ nanoscale increased from 2 to 5%, the response of electrode improved and when the ratio was more than 5%, the response decreased with larger background current, which is attributed to an increase in the resistance and double layer capacitance of the modified electrode, as a consequence of the decrease in the ratio of carbon nanotubes and resulted in poor measure for H_2O_2 (Fig. 4B). Therefore 20 μL of 5% $Ni(OH)_2$ Nanoscale was chosen for the fabrication of the biosensor. CS because of its biocompatibility and bioadhension, played the roles of sustaining the natural structure of Mb and keeping good interaction with $Ni(OH)_2$, which enhanced the electron transfer process. The effects of various concentration of CS have also been studied (data are not shown). It is found that the film had poor mechanical stability with the concentration of Cs less than 0.5%, and large background current with the concentration of Cs larger than 0.7%. An optimum loading 10 μL of 0.5% Cs was used for subsequent experiment.

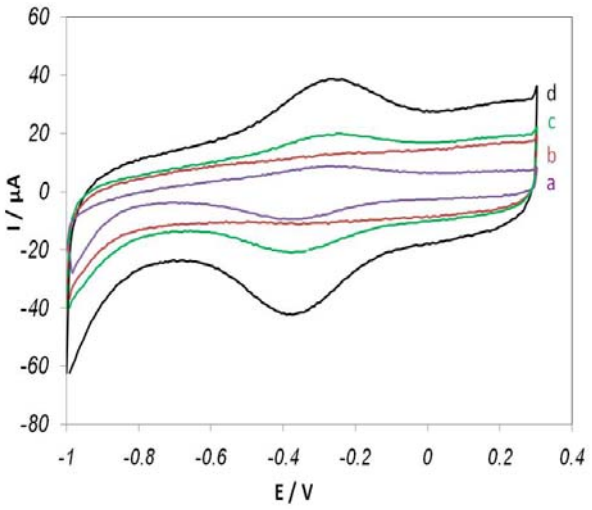

Fig. 3. CVs recorded in PBS (pH 7.5, 0.1M) at Cs/Mb/Ni(OH)2/GCE (a), $Ni(OH)_2$-MWCNTs/GCE (b), Cs/Mb/MWCNTs/GCE (c) and Cs/Mb/$Ni(OH)_2$-MWCNTs/GCE (d). Scan rate: 100 mV/s

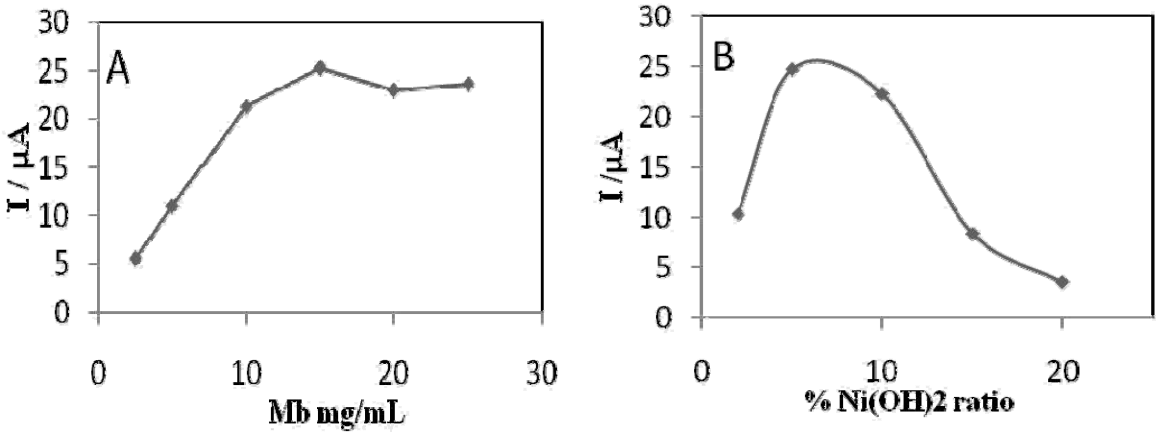

Fig. 4. A) Effect of the concentration of Mb on the biosensor response. Supporting electrolyte, 0.1 M pH 7.5 PBS. B) Effect of the ratio of NHNP on the biosensor response

3.4. Effect of pH solution

In most cases, protein redox behavior is often significantly dependent on the solution. The CV peaks of the modified electrode in 10 µM H_2O_2 were measured with well-defined peaks in the pH range from 4.0 to 9.5 (Fig. 5). As shown in Fig. 5a, the higher cathodic peak currents for H_2O_2 are resulted in buffer solution with pH 7.5. Further investigation of the dependence of peak potential upon pH, it is found that there is linear relationship between peak potential and pH, the regression equation is E^0(mV)=-66.0-43.0 pH (Fig. 5b). The slope value of -43.0 mV/pH is smaller than the theoretical value of -57.6mV/pH for a reversible proton coupled single electron transfer process which might be explained as the effect of the protonation states of trans ligands to the heme iron and amino acids around the heme [31, 32] or the protonation of water molecules coordinated to the central iron that may exist at different pH values [33]. This suggests that a quasi-reversible one-electron transfer accompanies a single-proton transfer between the electrode and the heme of Mb.

3.5. Effect of the scan rate

To obtain the kinetic parameters of Modified electrode the effect of scan rate was examined. From Fig. 6, it can be found that the peak currents increased with increasing of scan rate in 10–800 mV/s and the results show symmetrical anodic and cathodic peaks of approximately equal heights for Mb at different scan rates. The anodic and cathodic peak currents were linearly related to the scan rate (ν) (Fig. 6a). This result indicated that Mb immobilized on the electrode undergoes a quasireversible electron transfer with the MWCNTs and $Ni(OH)_2$ nanoscale islands. The electrochemical behavior of Mb immobilized on MWCNTs-$Ni(OH)_2$ nanoscale film was a surface-controlled process [32]. It is also found that peak potential varied linearly with the scan rate in the range of 50–600 mVs^{-1} (Fig. 6b,c), while the formal potential kept almost unchanged. The regression equation was

E_{pc}=−0.1068 log ν –0.5 with a coefficient of 0.9983. According to Laviron equation [34]. The relationships of E_p with log ν were calculated and shown in Fig. 4c with two linear equations. Form the slope and the intercept, the value of n and α were got as 1.11 and 0.49, respectively. When $n\Delta E_p \leq 200$mV, the electron transfer rate K_s can be estimated with the Laviron's equation $K_s=\alpha\, nFv/RT$ [35]. An apparent surface electron transfer rate constant, K_s=2.13 s^{-1}, was estimated. The results also show that the integration of $Ni(OH)_2$ and MWCNTs can provide a remarkable synergistic augmentation of biosensor performance. The estimated value is in the controlled range of surface-controlled quasi-reversible process.

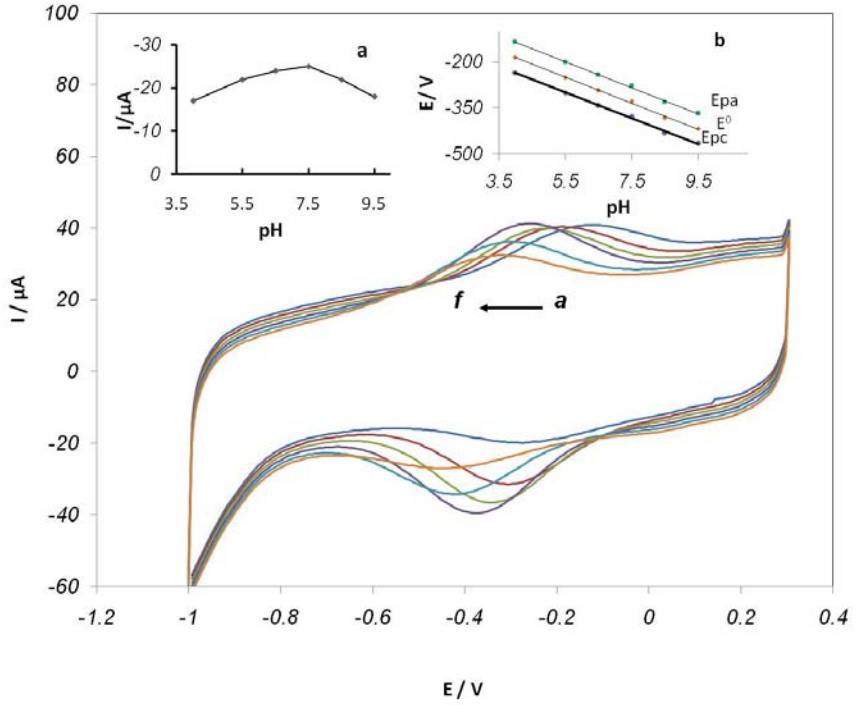

Fig. 5. Cyclic voltammograms of Cs/Mb/NHNP-MWCNTs/GCE in 0.1 M PBs at different pHs.(curves a–f: pH =4, 5.5, 6.5, 7.5, 8.5, 9.5) in the presence of 10 μM of H_2O_2 and scan rate: 0.1 V s^{-1}. a), plot of peak current *vs*. pH values, b) Plots of E *vs*. pH

3.6. Electrocatalytic activity of H_2O_2 on the Biosensor

The electrocatalytic effect of the electrode has also been investigated in the presence of different concentrations of hydrogen peroxide (Fig. 7a). As shown, with increasing H_2O_2 concentration, the reduction peak currents were increased and the peak potentials were shifted to more negative values. The decrease of overvoltage and increased peak current of hydrogen peroxide reduction confirm that $Ni(OH)_2$-MWCNTs film has high catalytic ability for H_2O_2 oxidation. The catalytic peak currents are proportional to the concentration of H_2O_2 and the linear regression equation for the concentration range from 0.5–500 μM is obtained as I(μA)=-0.631C(μM)-18.5, R^2=0.9995. The detection limit is estimated to be 0.285 μM

when the signal to noise ratio is 3. It can be inferred from these results that the presence of the composite film on the surface of GC electrode facilitates the detection of hydrogen peroxide at low concentration level.

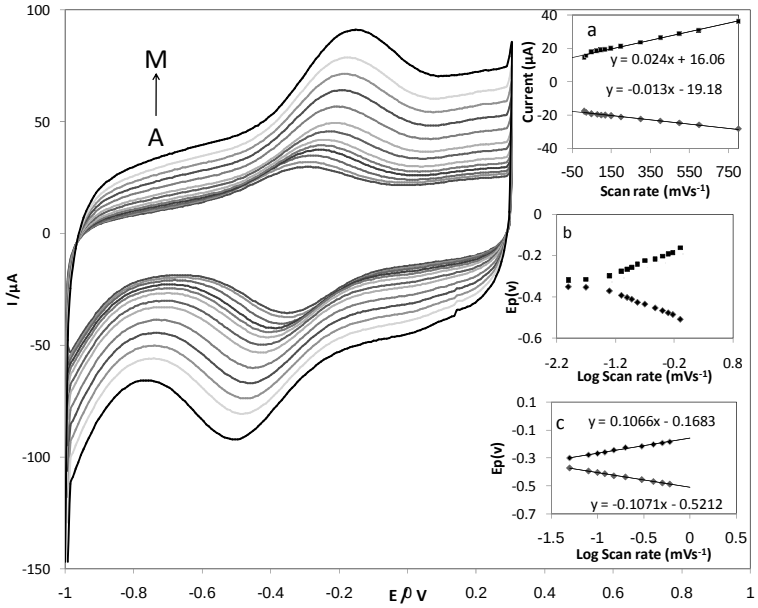

Fig. 6. CVs of Cs/Mb/Ni(OH)$_2$-MWCNTs/GCE at different scan rates (from A to M) 0.01, 0.02, 0.05, 0.08, 0.1, 0.12, 0.15, 0.2, 0.3, 0.4, 0.5, 0.6 and 0.8 V s^{-1}. Insets: (a) dependence of peak currents *vs*. scan rate, (b) dependence of potential *vs*. logarithm value of scan rate and (c) Magnification of the same plot for high scan rate

The electrocatalytic reduction of hydrogen peroxide at Cs/Mb/Ni(OH)$_2$-MWCNTs/GCE was also studied by amperometry i-t curve. The potential dependence of amperometric signal was tested in the range from 0 to -0.60 V. The steady-state reduction current increased as the applied potential decreased from 0 to -0.30 V, which was due to the increased driving force for the fast reduction of H_2O_2 at low potential. So the value of -0.3 V was selected as optimum working potential. Fig. 7b illustrates a typical amperometric response of the Mb sensor at-0.30 V on successive step changes of H_2O_2 concentration to a continuous stirring 10 mL PBS solution under the optimized conditions. The modified electrode achieved 95% of steady-state current within 5 s. This result shows that the response time of the sensor is short. The current had a linear relationship with the concentration of H_2O_2. With Application of the method two linear ranges were obtained. The first linear dynamic range was from 0.4 μM to 9 μM, with a calibration equation of I_p(μA)=-0.258c (μM)+0.0121, R^2=0.9987, n=10 and the second linear dynamic range was between 9 μM to 702 μM with a calibration equation of I_p(μA)=-0.245c (μM)+0.0146, R^2=0.9981, n=10. A detection limit of 0.08 μM (S/N=3) was obtained. When the concentration of H_2O_2 is higher than 702 μM, a response plateau in

calibration curve is observed, showing the characteristics of the Michaelis–Menten kinetic mechanism. It can be obtained from the electrochemical version of the Lineweaver–Burk equation [36]. The K_M value was determined by analysis of the slope and intercept for the plot of the reciprocals of the cathodic current versus H_2O_2 concentration. The K_M value of the H_2O_2 biosensor was determined by steady-state amperometric response and found to be 64.2 μM. The value shows that the immobilized Mb retains its bioelectrocatalytic activity and possesses a high biological affinity toward H_2O_2 .

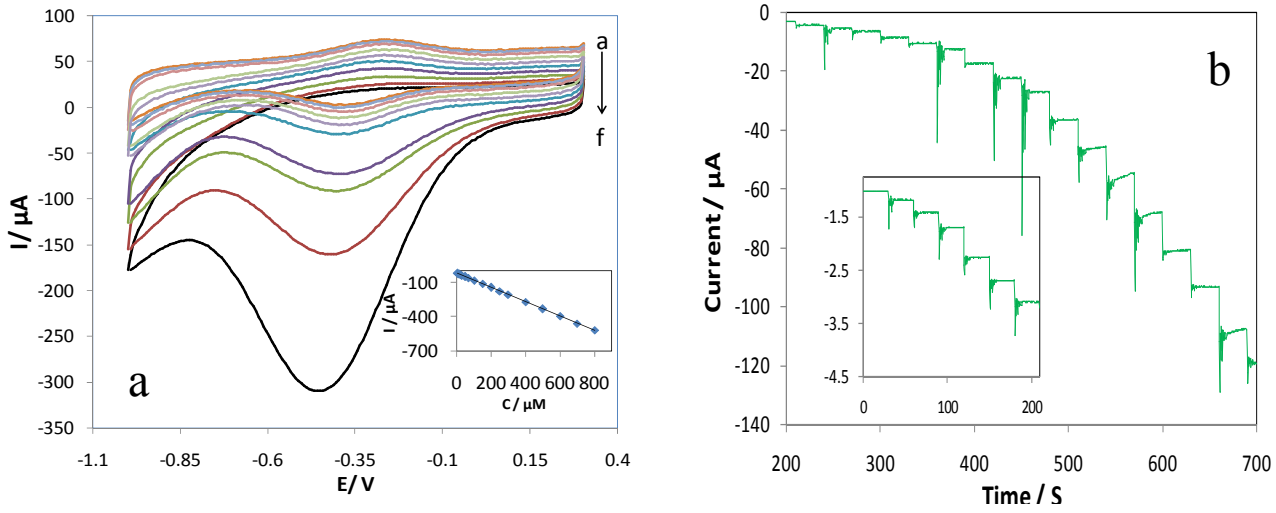

Fig. 7. Cyclic voltammetric response of the biosensor with different concentrations of H_2O_2 at a scan rate of 0.1 V s^{-1}. The H_2O_2 concentrations are as follows (a–f): 0, 0.5, 1, 2.5, 5, 10, 25, 50, 100 and 200 respectively (a), Typical current–time response to the successive additions of different concentrations of H_2O_2 at an applied potential of −0.3 V in the time intervals of 30 s from 9-702 μM (Inserts: From 0.4-9 μM)(b)

3.7. Repeatability and stability of the H_2O_2 biosensor

The biosensor shows good repeatability for the determination of H_2O_2 concentration in its linear range. The relative standard deviation (R.S.D.) is 2.8% for 15 successive assays at the H_2O_2 concentration of 10 μM. The stability of the proposed biosensor was investigated. After 100 cyclic runs, the voltammetric response to 10 μM H_2O_2 almost remained 94.8% of the initial response (data not shown). The storage stability of the proposed biosensor was also studied. When not in use, the electrode was suspended above PBS at 4 ^oC in a refrigerator. The response to 10 μM H_2O_2 was tested intermittently. After 7 and 15 days at 4 ^oC, the biosensor retained 92.1% and 90.4% of its initial response current, respectively.

3.8. Selectivity of developed H_2O_2 biosensor

The influences of common interfering species in presence of 10 μM H_2O_2 were investigated, and the results confirmed that interfering species did not significantly influence the height of the peak currents for H_2O_2.The tolerance limit was defined as the maximum concentration of the interfering substance that causes an error less than 10% for determination of H_2O_2. It was found that a 500-fold excess of NADH, 450-fold excess of glucose, 350-fold excess of Uric acid, 300-fold excess of sucrose, 250-fold excess of oxalic acid and citric acid, 220-fold excess of ascorbic acid, 200-fold excess of folic acid and $CaCl_2$ did not interfere with the measurement of H_2O_2.

3.9. Real sample analysis

In order to investigate the possibility of using the prepared biosensor, it was applied to the determination of H_2O_2 in blood serum samples and also a commercial oxidant solution. The actual concentration of H_2O_2 in the oxidant solution was determined by the $KMnO_4$ titration method [31] and also by using the recommended procedure in this work. The results are presented in Table 1 (n=3), which shows that there is a very good agreement between the results obtained for the commercial oxidant solution by the proposed sensor and those obtained by the potassium permanganate titration method, which was employed as the reference method.

Table 1. Result of analysis of H_2O_2 in real samples

Sample	added(μM)	found*(μM)	Recovery	RSD(%)
blood serum	-	0	-	-
	25	25.2	100.80	3.4
	50	49.8	99.60	3.3
	100	99.2	99.20	3
oxidant**	-	105.4	-	-
	25	134	102.76	4.3
	50	155	99.74	4
	100	209	101.75	3.2

*Average of five determinations at optimum conditions

**The concentration found by $KMNO_4$ titration method was 103.5 μM

Table 2. Comparison of the proposed electrode for H_2O_2 with other types of nanocomposite material modified electrode

Electrode	methode	linear range (μM)	Detection Limit μM)	K_s (s^{-1})	K_m^{app} (μM)	References
PVA/Clay/Hb/CILE	CV	7.5- 100	2	0.54	56.26	[37]
Cat–NiO/GCE	CA	1-1000	0.6	3.7	960	[38]
Hb-CdTe-CS/GCE	CA	7.44-6950	2.23	1.36	181	[16]
Cat-MWCNTs/GCE	CA	10-100	1	80	420	[39]
Mb-SWCNTs-CTAB	CA	61.8-507	18.5	NR	61000	[40]
Mb/MWCNTs/Cs/GCE	CA	37.9-550	NR	NR	1070	[41]
Nafion/Mb/IL/GCE	CA	1-180	0.14	NR	22.6	[42]
Nafion/Mb/MWCNTs/CILE	CV	8-1960	6	NR	0.181	[43]
Nafion/Mb/IL/PtNPs/MWCNTs/GCE	CA	0.5-210	0.1	0.41	69	[44]
Cs/Mb/Ni(OH)$_2$-MWCNTs/GCE	**CV** **CA**	**0.5 – 500** **0.4-702**	**0.285** **0.08**	**2.13**	**64.2**	**This work**

NR=Not reported, HRP=horseradish peroxidase, PVA: polyvinyl alcohol, CdTe=cadmium telluride nanoparticles, Cat=catalase, CTAB=cetyltrimethyl ammonium bromide

4. CONCLUSIONS

In this paper, direct electrochemistry of Mb was immobilized on nickel hydroxide nanoparticles-chitosan-carbon nanotubes-modified electrode. The modified electrode was fabricated by a layer-by-layer casting method, and the resulting electrode exhibited a good electrocatalytic performance to H_2O_2 because of the combining of $Ni(OH)_2$ and MWCNTs. Comparisons between the analytical characteristics of the proposed electrode with other types of nanocomposite material modified electrode for H_2O_2 determination are listed in Table 2. The simple fabrication procedure, high speed, reproducibility, high stability, wide linear dynamic range, low detection limit, high sensitivity, suggest that the proposed biosensor is an attractive candidate for practical applications.

Acknowledgments

The authors gratefully acknowledge the research council of Arak University for providing financial support for this work.

REFERENCES

[1] A. Riklin, E. Katz, I. Wiliner, A. Stocker, and A. F. Buckmann, Nature 376 (1995) 672.
[2] W. Zhang, and G. Li, Anal. Sci. 20 (2004) 603.
[3] Y. Usui, K. Sato, and M. Tanaka, Angew. Chem. Int. Ed. 42 (2003) 5623.
[4] J. Wang, Electroanalysis 13 (2001) 983.
[5] J. J. Gooding, Electrochim. Acta 50 (2005) 3049.
[6] S. K. Smart, A. I. Cassady, G. Q. Lu, and D. J. Martin, Carbon 44 (2006) 1034.
[7] J. Yang, and N. Hu, Bioelectrochem. Bioenerg. 48 (1999) 117.
[8] A. E. F. Nassar, Z. Zhang, N. Hu, J. F. Rusling, and T. F. Kumosinski, J. Phys. Chem. B 101 (1997) 2224.
[9] H. Sun, H. Ma, and N. Hu, Bioelectrochem. Bioenerg. 49 (1999) 1.
[10] H. Huang, N. Hu, Y. Zeng, and G. Zhou, Anal. Biochem. 308 (2002) 141.
[11] H. Li, S. Liu, Z. Dai, J. Bao, and X. Yang, Sensors 9 (2009) 8547.
[12] Y. Zhang, R. Yuan, Y. Chai, Y. Xiang, C. Hong, and X. Ran, Biochem. Eng. J. 51 (2010) 102.
[13] Q. Zhao, Z. Gan, and Q. Zhuang, Electroanalysis 14 (2002) 1609.
[14] M. Moreno-Manas, and R. Pleixats, Acc. Chem. Res. 36 (2003) 638.
[15] A. Roucoux, J. Schulz, and H. Patin, Chem. Rev. 102 (2002) 3757.
[16] Q. Xu, J. H. Wang, Z. Wang, H.Q. Wang, Q. Yang, and Y. D. Zhao, Anal. Lett. 42 (2009) 2496.
[17] T. J. Zhang, W. Wang, D. Y. Zhang, X. X. Zhang, Y. R. Ma, Y. L. Zhou, and L. M. Qi, Adv. Funct. Mater. 20 (2010) 1152.
[18] X. Kang, Z. Mai, X. Zou, P. Cai, and J. Mo, Anal. Biochem. 363 (2007) 143.
[19] C. Y. Liu, and J. M. Hu, Biosens. Bioelectron. 24 (2009) 2149.
[20] K. Ohnishi, Y. Einaga, H. Notsu, C. Terashima, N. Rao, S. G. Park, and A. Fujishima, Electrochem. Solid-State Lett. 5 (2002) D1.
[21] I. G. Casella, and M. Gatta, Anal. Chem. 72 (2000) 2969.
[22] Q. Li, L. S. Wang, B. Y. Hu, C. Yang, L. Zhou, and L. Zhang, Mater. Lett. 61 (2007) 1615.
[23] G. r. Fu, Z. a. Hu, L. j. Xie, X. q. Jin, Y. l. Xie, Y. x. Wang, Z. y. Zhang, Y. y. Yang, and H. y. Wu, Int. J. Electrochem. Sci. 4 (2009) 1052.
[24] T. You, O. Niwa, Z. Chen, K. Hayashi, M. Tomita, and S. Hirono, Anal. Chem. 75 (2003) 5191.
[25] A. Safavi, N. Maleki, and E. Farjami, Biosens. Bioelectron. 24 (2009) 1655.
[26] G. Xiao-yan, and D. Jian-cheng, Mater. Lett. 61 (2007) 621.
[27] X. L. Li, J. F. Liu, and Y. D. Li, Mater. Chem. Phys. 80 (2003) 222.
[28] D. Chen, and L. Gao, Chem. Phys. Lett. 405 (2005) 159.

[29] M.G. Peter, J. Macromol. Sci. Pure Appl. Chem. 32 (1995) 629.
[30] G. S. Lai, H. L. Zhang, and D. Y. Han, Sens. Actuators B 129 (2008) 497.
[31] A. I. Vogel, 5th ed., Longman, New York (1989).
[32] A. J. Bard, and L.R. Faulkner, 2th ed., John Wiley and Sons, Chichester, Brisbane, Toronto, New York (2001).
[33] I. Yamazaki, T. Araiso, Y. Hayashi, H. Yamada, and R. Makino, Adv. Biophys. 11 (1978) 249.
[34] E. Laviron, J. Electroanal. Chem. Int. Electrochem. 52 (1974) 355.
[35] E. Laviron, J. Electroanal. Chem. Int. Electrochem. 101 (1979) 19.
[36] A. K. Upadhyay, T. W. Ting, and S. M. Chen, Talanta 79 (2009) 38.
[37] N. Hui, R. f. Gao, X. q. Li, W. Sun, and K. Jiao, J. Braz. Chem. Soc. 20 (2009) 252.
[38] A. Salimi, E. Sharifi, A. Noorbakhsh, and S. Soltanian, Biophys. Chem. 125 (2007) 540.
[39] A. Salimi, A. Noorbakhsh, and M. Ghadermarz, Anal. Biochem. 344 (2005) 16.
[40] H. Xu, H. Xiong, Q.X. Zeng, L. Jia, Y. Wang, and S. F. Wang, Electrochem. commun. 11 (2009) 286.
[41] L. S. Duan, Q. Xu, F. Xie, and S. F. Wang, Int. J. Electrochem. Sci. 3 (2008) 118.
[42] A. Safavi, and F. Farjami, Anal. Biochem. 402 (2010) 20.
[43] W. Sun, X. Li, Y. Wang, X. Li, C. Zhao, and K. Jiao, Bioelectrochem. 72 (2009) 170.
[44] A. Babaei, D. J. Garrett, and A. J. Downard, Int. J. Electrochem. Sci. 7 (2012) 3141.